

Modelling rapidly rotating stars

Daniel Reese

Applied Maths Department, University of Sheffield, Hicks Building, Hounsfield Road, S3 7RH

E-mail: d.reese@sheffield.ac.uk

Abstract. Recent interferometric observations have drawn attention to the effects of rapid rotation on stellar structure. Consequently, a number of 2D models and pulsation codes have been and are being developed in order to gain a better understanding of such stars. These have shed light on effects like centrifugal deformation, gravity darkening, differential rotation and the transport of chemical elements and angular momentum. Pulsation modes within these stars have a different geometrical structure, characterised by a new organisation of the frequency spectrum, as shown by eigenmode calculations and ray dynamics.

1. Introduction

Recent observations have revealed the drastic effects of rapid rotation on stellar structure. For instance, Domiciano de Souza et al. (1) have shown that Achernar is highly oblate due to centrifugal deformation. Naturally, this caught the attention of those in the theoretical community (2). Further observations have revealed more subtle effects like gravity darkening (3; 4; 5; 6). Also, various spectroscopic surveys have shown that many stars have large equatorial velocities (*c.f.* 7, and references therein). This naturally leads to the question as to what is involved when modelling and dealing with such stars.

In what follows, we will look at two themes, namely, modelling rapidly rotating stars and understanding how they pulsate. Section 2 discusses some of the latest stellar models and the complications introduced by rapid rotation. Section 3 describes recent progress in calculating and understanding pulsation modes in such stars. This is then followed by a conclusion.

2. Stellar models

2.1. Physical phenomena

In order to be as realistic as possible, models of rapidly rotating stars need to include a number of new phenomena which are not present in non-rotating stars. These include:

- (i) **Centrifugal deformation:** the centrifugal force counteracts gravity, causing the equatorial region to expand. Consequently, rapidly rotating stars are oblate and cannot be described by a one-dimensional spherically symmetric model. If one introduces differential rotation, it is possible to obtain highly deformed configurations, like the one shown in Figure 1, taken from (8). The recent observations of Achernar (1; 9) have shown a degree of oblateness which may be difficult to achieve using uniform rotation and thus require differential rotation (2).
- (ii) **Gravity darkening:** according to the von Zeipel law, $g_{\text{eff}} \propto F \propto T_{\text{eff}}^4$ where g_{eff} is the effective gravity (which includes the centrifugal force), F the luminous flux and T_{eff} the effective blackbody temperature corresponding to F (10). As a result, since the effective

gravity is lower in the equatorial region, the luminous flux and the effective temperature are also lower. Another, way of looking at this is that the poles are closer to the stellar core and therefore hotter (6). More realistic models (11), as well as observations (6), do not strictly obey the von Zeipel law as it was derived for a barotropic stellar structure¹.

- (iii) **Baroclinic flows:** in stellar radiative zones of rotating stars, it is not possible to satisfy both the hydrostatic and energy equations. This was first indicated when von Zeipel found that assuming a uniform rotation rate, which in the absence of other fluid flows leads to a barotropic stellar structure, gives rise to an unusual (and unphysical) energy generation rate (10). This problem arises because heat radiates in an isotropic manner (*i.e.* isotherms tend to be spherical) which conflicts with the tendency to oblateness due to the centrifugal force (12). As a result, the hydrostatic equation needs to be replaced by a “hydro-stationary” equation, *i.e.* it must include a permanent baroclinic flow which can incorporate differential rotation and meridional circulation. Furthermore, the stellar structure cannot be barotropic. (13) gives a more detailed explanation of baroclinicity and its historical development.
- (iv) **Transport processes:** differential rotation resulting from baroclinicity most likely leads to turbulence which will then play an important role in the different transport processes (14). Over time, these modify the distribution of different chemical species and angular momentum and, as a result, affect stellar evolution (15). Also, gravity waves are expected to carry angular momentum and thus participate in the transport processes (*c.f.* Mathis, these proceedings).

2.2. Recent models

In order to understand how the previously mentioned phenomena affect stars, their structure and their evolution, a number of models have been and are being developed. In what follows we will only look at recent models. For a review of older models, one can look at (16).

About 10 years ago, a series of seven articles (17; 18; 19; 20; 15; 21; 22) was started, based on the ideas of Zahn (14). These articles assume that the rotation profile is shellular (*i.e.* it is constant on equipotential surfaces) due to anisotropic turbulence which is stronger in the horizontal direction. This allows them to investigate the effects of rotation using a 1D formalism. They look at mass loss through anisotropic stellar winds and the transport of angular momentum and chemical species, and see how it affects a star’s evolution in the HR diagram, its lifetime and its chemical yields. Using their models, they explain abundance anomalies in OBA stars, the ratio of blue supergiants to red ones in the Small Magellanic Cloud and several other observations (*c.f.* 23, and references therein).

Prompted by the observations of Achernar, Jackson et al. (2) came up with models based on a revised version of the Self-Consistent Field (SCF) method (24). This was followed by two more articles which explain the method and its results in greater detail (25; 8). These models are characterised by a conservative rotation law, *i.e.* a rotation profile which only depends on the distance to the rotation axis. As a result, the centrifugal force derives from a potential which can be grouped with the gravitational potential to form an effective or total potential. By also assuming that there are no other fluid flows besides rotation, they obtain a barotropic structure in which the different thermodynamic quantities only depend on the total potential. As a result, the problem is essentially 1D like in the previous case, apart from the resolution of Poisson’s equation. Using their models, they investigate how rotation alters stellar shape and structure (*c.f.* Figure 1), deepens convective envelopes, shrinks convective cores and causes stars to mimic lower mass non-rotating stars in the HR diagram.

¹ A stellar structure is barotropic if isodensities, isobars and isotherms coincide.

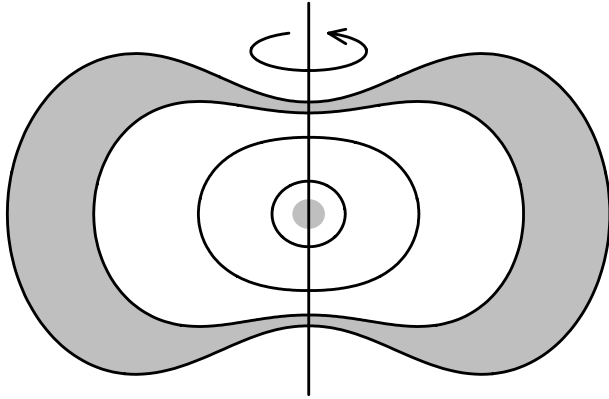


Figure 1. Cross-section of a $2 M_{\odot}$ rotating star. Note the highly deformed configuration due to differential rotation. The shaded areas correspond to convection zones. Taken from (8).

Other models of interest include those of Roxburgh (26; 27). The models in (26) are uniformly rotating barotropic models, quite similar to those mentioned in the previous paragraph. In the later article, Roxburgh takes a very different and original approach, in which a 1D model is converted into 2D. This is done by imposing the density and composition profile from the 1D model along a radial cut, choosing an arbitrary 2D rotation profile (which can be non-conservative), and propagating the solution to the rest of the 2D model by solving the hydrostatic and Poisson's equations. The drawback to this method is that the energy equation is not solved and therefore the star is not necessarily in radiative equilibrium. Nonetheless, the acoustic properties of such models can be investigated as they are governed by the hydrostatic structure.

Finally, there is the ESTER² project which seeks to do 2D stellar evolution while fully taking into account the effects of rotation. One of the first steps in this project was to investigate the baroclinic flows which occur in a spherical boussinesq model (28) and to try to deduce some general properties of such flows. This has then been followed by a more realistic model which fully takes into account the compressibility of the fluid but is still confined to a spherical container (11). Using this approach, Espinosa Lara and Rieutord are able to predict the differential rotation profile deduced from the baroclinic flow (*c.f.* Figure 2). Further results include a departure of the luminous flux and temperature from the von Zeipel law and the appearance of a convectively unstable zone confined to the equatorial region.

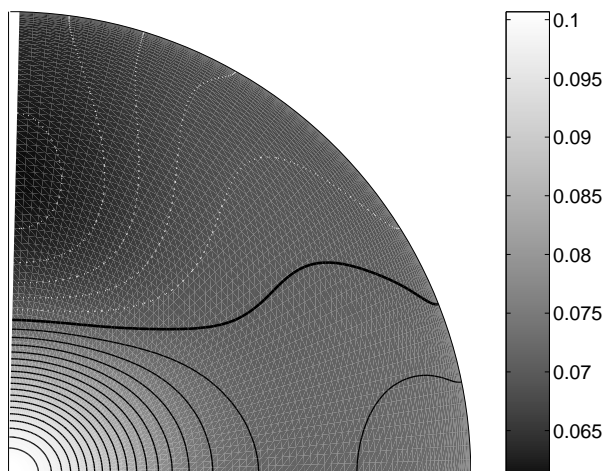


Figure 2. Differential rotation profile resulting from baroclinic effects. The lines correspond to iso-contours of the rotation rate, the thick line being the average rotation rate. The poles rotate more slowly than the equator, as indicated by the white dotted lines. Taken from (11).

Nonetheless many uncertainties remain in modelling such stars (*c.f.* 16, for a list of some of these). This is illustrated by the fact that none of the preceding models implement the same rotation rate. It is therefore necessary to obtain observational constraints in order to refine such models. Asteroseismology places some of the strongest constraints on stellar structure and is therefore the most logical place to look.

3. Stellar pulsations

The study of pulsation modes in rapidly rotating stars is rather difficult for several reasons. Because of the loss of spherical symmetry, pulsation modes no longer reduce to a single spherical harmonic but are the solution of a 2D eigenvalue problem, which make them much harder to calculate. Furthermore, the geometry of modes and the pattern of frequencies in the pulsation spectrum are quite different from the spherical (or slowly rotating) case and therefore poorly understood. For these reasons, successful asteroseismic inferences have so far been limited to slowly rotating stars. In order to go to higher rotation rates, much progress is needed in understanding pulsation modes and their properties.

Historically, two main approaches have been used to study the effects of rotation on stellar pulsations. The first is the perturbative method in which the effects of rotation are treated as a correction to the non-rotating case. Naturally, this method is limited to relatively slow rotation rates (29). The second method is the complete approach, in which the 2D problem is solved directly. Consequently, it can be applied to arbitrary rotation rates. Due to its complexity and the fact that it is numerically more demanding, it has not yet been used as a means of interpreting pulsations in rapidly rotating stars. A more detailed explanation of both methods as well as a list of key articles can be found in (7). In what follows we will focus on the latest developments in the study of acoustic modes using the complete method.

3.1. The frequency spectrum

As was stated earlier, the spectrum of frequencies at rapid rotation rates is quite different than what is obtained for slowly rotating stars. The frequency spectrum at slow rotation rates is characterised by frequency multiplets and an asymptotic pattern based on the large and small frequency separations. At rapid rotation rates, the frequency multiplets overlap and are therefore no longer recognisable, and the small frequency separation is no longer small. Nonetheless, an asymptotic pattern can be found for low degree modes of polytropic models, and is given by the following formula, in a co-rotating frame (30; 31):

$$\omega_{n,\ell,m} = n\Delta_n + \ell\Delta_\ell + |m|\Delta_m + \alpha^\pm \quad (1)$$

The quantum numbers (n, ℓ) are carried over from the non-rotating counterparts to these modes but are not indicative of mode geometry (*c.f.* Section 3.2). This formula bears some resemblance to Tassoul's asymptotic formula (32) except that the ratio Δ_n/Δ_ℓ is no longer 2 (which explains the loss of the small frequency separation), a supplementary term appears for non-axisymmetric modes, and the constant α "splits" into 2 constants α^+ and α^- , one for modes which are symmetric with respect to the equator, and the other for antisymmetric modes. The term $|m|\Delta_m$ uses the absolute rather than algebraic value of m because it is primarily due to the centrifugal force, which does not depend on the sign of m . Numerically, it turns out that the increment Δ_m is negative as opposed to Δ_n and Δ_ℓ .

3.2. The geometry of pulsation modes

The departure of the frequency spectrum from the usual structure goes hand in hand with a strong modification of mode geometry at rapid rotation rates. Low degree pulsation modes take on an elongated shape which circumvents the equatorial regions, as can be seen in Figure 5.

Consequently, as shown in (33), a more appropriate set of quantum numbers is $(\tilde{n}, \tilde{\ell}, m)$ where \tilde{n} is the number of nodes along the mode's elongated structure, $\tilde{\ell}$ the number of nodes parallel to this structure and m the usual azimuthal order. This is illustrated in the last frame of Figure 3. In what follows, we will call “pseudo-radial” the nodes along the mode's structure and “pseudo-latitudinal” the parallel nodes.

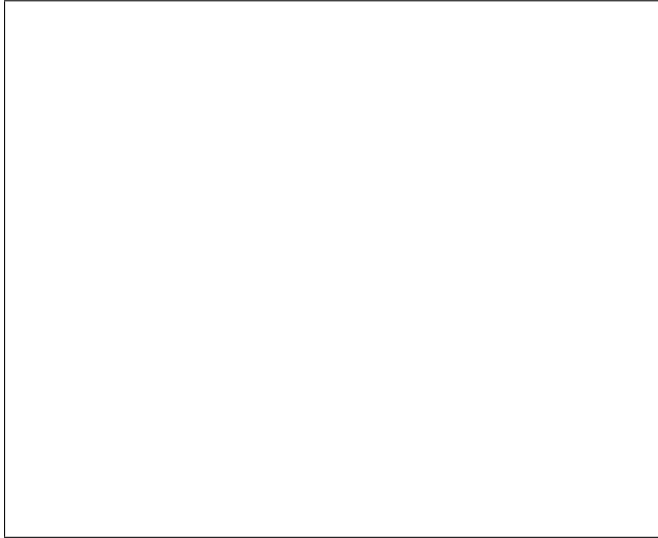


Figure 3. First frame in a sequence which shows how the $(n, \ell, m) = (5, 3, 0)$ mode at $\Omega = 0$ becomes the $(\tilde{n}, \tilde{\ell}, m) = (11, 1, 0)$ mode at $0.84 \Omega_K$, where Ω_K is the Keplerian break-up rotation rate (the rest of the sequence is available here). The first and last frames indicate what the different quantum numbers represent.

In order to understand how $(\tilde{n}, \tilde{\ell}, m)$ relate to (n, ℓ, m) , it is necessary to follow a mode's evolution from $\Omega = 0$ to the rapid rotation regime. Figure 3 shows a sequence in which the $(n, \ell, m) = (5, 3, 0)$ mode transforms itself into the $(\tilde{n}, \tilde{\ell}, m) = (11, 1, 0)$ mode. As can be seen in the sequence, radial nodes transform themselves into pseudo-radial nodes. However, since we're counting the nodes from stellar surface to stellar surface, \tilde{n} is approximately twice n . In the same way the latitudinal nodes become pseudo-latitudinal nodes, except for the equatorial node which becomes a pseudo-radial node. These are half as numerous as their non-rotating counterparts, since they span both hemispheres. These observations lead to the following relationships between the different quantum numbers:

$$\tilde{n} = 2n + \varepsilon, \quad (2)$$

$$\tilde{\ell} = \frac{\ell - |m| - \varepsilon}{2}, \quad (3)$$

$$\varepsilon = \ell + m \bmod 2 \quad (4)$$

Using these new quantum numbers, Equation 1 can be rewritten as follows:

$$\omega_{n,\ell,m} = \tilde{n}\tilde{\Delta}_n + \tilde{\ell}\tilde{\Delta}_\ell + |m|\tilde{\Delta}_m + \tilde{\alpha}^\pm \quad (5)$$

where $\tilde{\Delta}_n = \Delta_n/2$, $\tilde{\Delta}_\ell = 2\Delta_\ell$, $\tilde{\Delta}_m = \Delta_\ell + \Delta_m$, $\tilde{\alpha}^+ = \alpha^+$ and $\tilde{\alpha}^- = \alpha^- + \Delta_\ell - \Delta_n/2$. Numerically, it turns out that $\tilde{\alpha}^+ \simeq \tilde{\alpha}^-$, so that the distinction between symmetric and antisymmetric modes is no longer necessary. Furthermore, $\tilde{\Delta}_m$ is positive. Both of these observations suggest that this alternate form is more relevant physically.

3.3. Ray dynamics

More insight can be gained into mode geometry and the frequency spectrum through ray dynamics. Ray dynamics is an asymptotic approach which applies in the high frequency limit,

when the mode varies on a much smaller length scale than the background equilibrium. Starting with an initial point and direction, ray trajectories within the star are calculated much like in geometric optics.

In order to study trajectories in a systematic way, it is useful to plot a Poincaré section. Figure 4, which is taken from (34), contains the intersection points $(\cos \theta, \sin \psi)$ between a predefined surface (located just beneath the stellar surface) and 150 ray trajectories, where θ is the colatitude, and ψ the angle between the ray and the normal to the surface at the intersection point. It is possible to recognise different regions in this diagram. The regions with large values of $|\sin \psi|$ (located in the upper and lower parts of the diagram) correspond to whispering gallery trajectories, like the one shown in the upper left corner. In between is a region which corresponds to chaotic trajectories. Within this chaotic region, there are a number of “islands” which correspond to periodic orbits like the ones shown in the lower left and upper right corners.

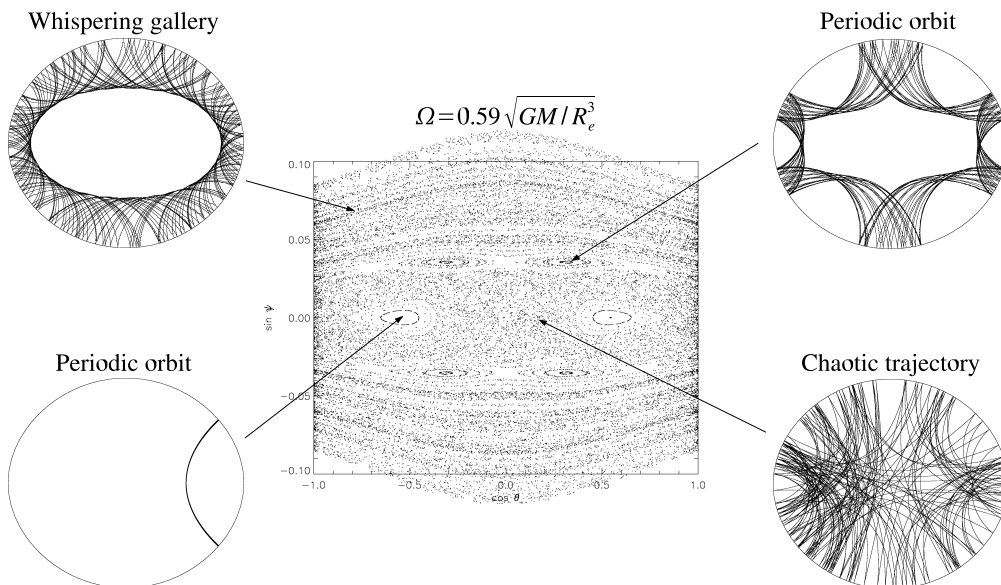


Figure 4. Poincaré section made up of the intersection points $(\cos \theta, \sin \psi)$ between a predefined surface just below the stellar surface and 150 trajectories, where θ is the colatitude and ψ the angle between the normal to the surface and the trajectory at the intersection point. Different regions correspond to different types of trajectories which are illustrated in the four corners. Taken from (34).

Of particular interest are the orbits with a period of two, like the one shown in the lower left corner of Figure 4. As can be seen in Figure 5, which is adapted from (35), these are the counterparts to the elongated modes discussed in the previous section. Lignières and Georgeot (33) push the analysis further by finding analytical formulae for $\tilde{\Delta}_n$ and $\tilde{\Delta}_\ell$ based on wave travel times along the ray’s path. By evaluating the analytical expression for $\tilde{\Delta}_n$ and comparing it with the value obtained numerically from the eigenfrequencies, they obtain an agreement to within 2%.

The other types of trajectories also have corresponding modes, the frequencies of which are given either by different asymptotic formulae or by a probability distribution in the case of chaotic modes (33). This correspondence can be established by projecting modes onto the Poincaré section by means of Husimi functions and seeing in which region they lie, thus providing

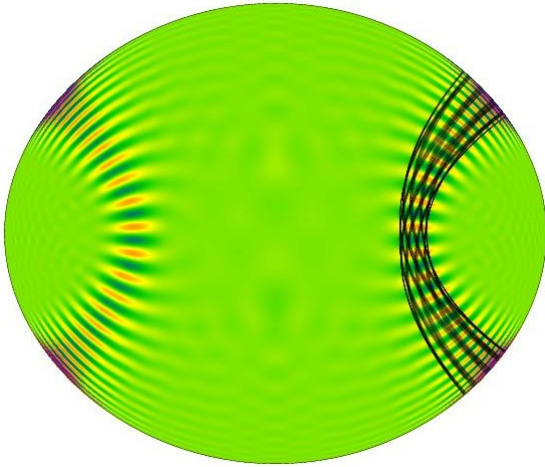


Figure 5. Ray trajectory superimposed on a low degree, high order pulsation mode (the mode is represented by a scaled version of the pressure perturbation). As can be seen, the trajectory overlaps very well with the mode’s location. Taken and adapted from (35).

a means of mode classification. In the case of non-chaotic modes, a direct comparison between the trajectories and mode geometry confirms this classification.

4. Conclusion

As can be seen, a lot of progress has been made in modelling the effects of rapid rotation both in stellar structure and pulsations. Yet given the difficulty of the problem, much work still remains before being able to accurately model such stars and correctly interpret their pulsations. This need for a better understanding is all the more pressing as observations progress and become more accurate. Spectacular advances in interferometry continue to challenge existing models, and asteroseismology ground networks and space missions provide pulsation data of unprecedented quality which require interpretation. Coming to grips with rapid rotation will provide a key element in the understanding of stars and their evolution and will doubtless raise many more questions.

Acknowledgments

I would like to thank Michel Rieutord and François Lignières for useful discussions on this subject. Participation of Daniel Reese at the HELAS II conference “Helioseismology, Asteroseismology, and MHD Connections” was supported by the European Helio- and Asteroseismology Network (HELAS). HELAS is funded by the European Union’s Sixth Framework Programme.

References

- [1] Domiciano de Souza A, Kervella P, Jankov S, Abe L, Vakili F, di Folco E and Paresce F 2003 *A&A* **407** L47–L50
- [2] Jackson S, MacGregor K B and Skumanich A 2004 *ApJ* **606** 1196–1199
- [3] Domiciano de Souza A, Kervella P, Jankov S, Vakili F, Ohishi N, Nordgren T E and Abe L 2005 *A&A* **442** 567–578
- [4] Peterson D M, Hummel C A, Pauls T A, Armstrong J T, Benson J A, Gilbreath G C, Hindsley R B, Hutter D J, Johnston K J, Mozurkewich D and Schmitt H 2006 *ApJ* **636** 1087–1097
- [5] Peterson D M, Hummel C A, Pauls T A, Armstrong J T, Benson J A, Gilbreath G C, Hindsley R B, Hutter D J, Johnston K J, Mozurkewich D and Schmitt H R 2006 *Nature* **440** 896–899 (*Preprint astro-ph/0603520*)

- [6] Monnier J D, Zhao M, Pedretti E, Thureau N, Ireland M, Muirhead P, Berger J P, Millan-Gabet R, Van Belle G, ten Brummelaar T, McAlister H, Ridgway S, Turner N, Sturmman L, Sturmman J and Berger D 2007 *Science* **317** 342–345 (*Preprint* arXiv:0706.0867)
- [7] Reese D 2007 *EAS Publications Series (EAS Publications Series vol 26)* pp 111–119
- [8] MacGregor K B, Jackson S, Skumanich A and Metcalfe T S 2007 *ApJ* **663** 560–572 (*Preprint* arXiv:0704.1275)
- [9] Kervella P and Domiciano de Souza A 2006 *A&A* **453** 1059–1066
- [10] von Zeipel H 1924 *MNRAS* **84** 665–683
- [11] Espinosa Lara F and Rieutord M 2007 *A&A* **470** 1013–1022
- [12] Zahn J P 1993 *Les Houches Summer School Proceedings (1987)* ed Zahn J P and Zinn-Justin J pp 565–615
- [13] Rieutord M 2006 *EAS Publications Series* **21** 275–295 (*Preprint* astro-ph/0608431)
- [14] Zahn J P 1992 *A&A* **265** 115–132
- [15] Meynet G and Maeder A 2000 *A&A* **361** 101–120 (*Preprint* astro-ph/0006404)
- [16] Rieutord M 2006 *SF2A-2006: Semaine de l’Astrophysique Francaise* ed Barret D, Casoli F, Lagache G, Lecavelier A and Pagani L pp 501–506
- [17] Meynet G and Maeder A 1997 *A&A* **321** 465–476
- [18] Maeder A 1997 *A&A* **321** 134–144
- [19] Maeder A and Zahn J P 1998 *A&A* **334** 1000–1006
- [20] Maeder A 1999 *A&A* **347** 185–193
- [21] Maeder A and Meynet G 2000 *A&A* **361** 159–166 (*Preprint* astro-ph/0006405)
- [22] Maeder A and Meynet G 2001 *A&A* **373** 555–571 (*Preprint* astro-ph/0105051)
- [23] Meynet G and Maeder A 2005 *The Nature and Evolution of Disks Around Hot Stars (Astronomical Society of the Pacific Conference Series vol 337)* ed Ignace R and Gayley K G pp 15–+ (*Preprint* astro-ph/0409722)
- [24] Ostriker J P and Mark J W K 1968 *ApJ* **151** 1075–1088
- [25] Jackson S, MacGregor K B and Skumanich A 2005 *ApJS* **156** 245–264
- [26] Roxburgh I W 2004 *A&A* **428** 171–179
- [27] Roxburgh I W 2006 *A&A* **454** 883–888
- [28] Rieutord M 2006 *A&A* **451** 1025–1036 (*Preprint* astro-ph/0602040)
- [29] Reese D, Lignières F and Rieutord M 2006 *A&A* **455** 621–637 (*Preprint* astro-ph/0605503)
- [30] Lignières F, Rieutord M and Reese D 2006 *A&A* **455** 607–620 (*Preprint* astro-ph/0604312)
- [31] Reese D, Lignières F and Rieutord M 2007 *submitted*
- [32] Tassoul M 1980 *ApJS* **43** 469–490
- [33] Lignières F and Georgeot B 2007 *submitted*
- [34] Lignières F, Vidal S, Georgeot B and Reese D 2006 *SF2A-2006: Semaine de l’Astrophysique Francaise* URL <http://www2.iap.fr/sf2a/>
- [35] Vidal S 2006 *Ondes acoustiques et chaos dans les étoiles en rotation rapide* (Rapport de stage)